Mongolian Journal of Chemistry
www.mongoliajol.info/index.php/MJC

Fixed-bed adsorption of methylene blue solution onto sorghum grain husks

Abdellatif Cheiakh[1], Farid Halet[2], Salima Chergui[1], Farida Hamdache[1], Abdelmalek Chergui[3], Ahmed Reda Yeddou[1], Boubekeur Nadjemi[1]

[1]Department of Chemistry, ENS Kouba, Vieux kouba 16050, Algiers, Algeria
[2]Department of Biology, University M'Hamed Bougara Boumerdesx, Boumerdes 35000, Algeria
[3]National Polytechnic School of Algiers, El-Harrach 16200, Algiers, Algeria

Corresponding author: abdellatif.cheiakh@g.ens-kouba.dz; ORCID: https://orcid.org/0009-0004-7019-4688

Received: 05 January 2026; revised: 24 May 2026; accepted: 02 June 2026

ABSTRACT

This work contributes to the development and valorisation of natural adsorbents for use in industrial wastewater treatment processes. Sorghum grain husks, collected as agricultural waste from southern Algeria, were tested as an adsorbent to remove methylene blue from water using a fixed-bed column. Fourier transform infrared spectroscopy, point of zero charge, and scanning electron microscopy were used to assess the raw sorghum husk. The breakthrough curves were obtained at various values of the following parameters: bed height, flow rate, initial methylene blue concentration, and Hydrogen potential of solution. At an alkaline medium, the best methylene blue adsorption performance was observed. In a fixed-bed adsorption column, the highest uptake of methylene blue was 39.86 mg/g. Hydrochloric acid (0.1N) was used in regeneration tests for the fixed bed to enable multiple reuses of the natural adsorbent material. Both the Thomas and Yoon-Nelson models were used to find kinetic parameters.

Keywords: Methylene blue, raw sorghum husk, fixed bed column, adsorption

INTRODUCTION

Cationic dyes are used by many industries such as wool, plastics, pharmaceuticals, colouring paper, textiles, dyeing cottons, tannery, cosmetics, and paint [1]. During the textile dyeing process, approximately 13% of the used dyes is lost [2]. As a result, industrial wastewater contaminated with these types of dyes has endangered both human health and the environment [3]. These derivatives products can be very toxic; they can have mutagenic and carcinogenic effects on aquatic life and pose risks to human health [4], Methylene blue is one model of these basic dyes. It is a common colorant mostly used for silk or cotton [5]. Methylene is typically detectable even at low concentrations and resistant to natural biological wastewater treatment because of their complex molecular structures and synthetic origin [6]. Methylene can lead to reduced renal blood flow, skin and eye irritation, vomiting, and lowered cardiac output and mesenteric blood flow [7], Therefore, removing this dye from water is crucial. Different biological, chemical and physical treatment processes have been adopted to eliminate methylene blue and other dyes from industrial effluents such as, oxido- reduction [8], photocatalytic degradation [9, 10], biodegradation [11], electrolysis [12], electro-coagulation [13], foam flotation [14], ozonation [15], ion exchange [16], membrane filtration [17], and biosorption [18]. All these methods have their limitations and advantages. Adsorption offers a desirable and less expensive alternative to these conventional therapies [19]. For this purpose, various materials have been tested, including carbon nanotubes [20], metal oxides [21], polymers [22], nanocomposites and nanoparticles [23], as well as biological biomass [24]. Activated carbon is the most adsorbent used for wastewater treatment containing methylene blue [25]. This is because of its elevated specific surface area and large porous volume to adsorb a large amount of pollutant [26]. However, activated carbon is a high-cost adsorbent due to its complicated regeneration process and the complex chemical and physical modifications required for its production [27]. In recent years, several researches have investigated

alternative low-cost adsorbents such as agricultural waste [28], pine tree leaves [29], pine cone biomass [30], fallen Platanus leaves [31], date stones [32], and magnetic corn straw [33]. Several sorghum cultivars can be grown in southern Algeria, where irrigation often relies on saline subsurface water and the average monthly temperature (45.2 °C) is exceptionally high [34]. Sorghum is cultivated as a food as a food crop for human consumption. Until recently, sorghum stalks from locally grown varieties were primarily used as a livestock feed residue, but its grains waste are not consumable parts of sorghum. This work aims to demonstrate the use of sorghum husk as an effective material for removing dyes from water. Prior research on batch adsorption helped determine the maximum adsorption capacity and offered insightful information about the effectiveness of a contaminant-biosorbent system. Nevertheless, the results collected for batch system are typically not appropriate to an adsorptive fixed-bed system, where the time of contact isn't long enough to reach equilibrium [35]. Consequently, further investigations into continuous adsorption are required to conduct equilibrium research using thereby facilitating the transition toward large-scale industrial applications. There is not much information available about continuously removing pollutants using a fixed bed column. Fixed-bed column adsorption is technique used for the continuous removal of pollutants from wastewater. In this process, the contaminated solution flows through a column packed with an adsorbent material, where the pollutants are retained on the surface of the adsorbent until saturation is reached. Column performance is generally evaluated using breakthrough curves, which provide important information on adsorption capacity, mass transfer, and operational lifespan. This study aimed to test whether sorghum grain husks can be used as an adsorbent in a fixed bed column to remove methylene blue from water. The optimization of the adsorption process has involved studying the effects of several parameters, including Hydrogen potential (pH), flow rate, bed height and initial concentration of methylene blue. The column's performance was investigated using the Yoon-Nelson and Thomas kinetic models. Testing was also done on the fixed-bed regeneration to see if the adsorbent could be reused.

EXPERIMENTAL

Adsorbent preparation: Husk of Sorghum grains was collected from the Insalah region (south of Algeria). It was cleansed with tap water to remove any soluble contaminants from its surface, and then dried in ambient air for two days. An electric grinder has been used to break down the components into small particles. Following this step, the husk sorghum particles was subjected to successive washing cycles with hot distilled water (60-80 °C). The process was maintained until a clear effluent was obtained and the pH stabilized, ensuring the complete removal of leachable organic compounds. The material was then dried in an oven at 60 °C for 48 hours. Finally, the sorghum grains husks were sieved to achieve a particle size ranging from 400 to 500 μm. The material obtained is noted RSH (Raw Sorghum Husk). It was kept in a desiccator for use in the different experiments.

Adsorbent characterization: *Point of zero charge:* The zero-charge pH of the RSH was determined according to the following procedure: 50 mL of a 0.01 mol/L KNO_3 aqueous solution was placed in several Erlenmeyer flasks. The pH value in each flask was adjusted between 2 and 12 by adding NaOH or HCl (0.05 N) solutions. Then, a RSH mass of 0.2 g was added to each solution, and the flasks were carefully closed. After 24 hours, the final pH was measured using a pH Meter (HANNA/PH211).

Fourier transform infrared spectrometry analysis: To know the nature of the organic functions found on the surface of the adsorbent, infrared spectrometry has been applied (SHIMADZU FTIR-8400). The range of wave numbers under investigation was 500-4000 cm^{-1}.

Scanning electronic microscopy: The raw sorghum husk's morphology and microstructure were examined using a scanning electron microscope (SEM) (ZEISS XL30). Images were acquired before and after the adsorption process.

Specific surface area and pore volume: The BET specific surface area and porosity of the RSH adsorbent were determined from nitrogen adsorption-desorption isotherms (at 77 K) using a NOVA 2000 Quantachrome automatic analyzer.

Adsorbate preparation: The anhydrous cationic dye methylene blue, 3.7-bis Dimethylamino-phenazathionium chloride was obtained from Biochemopharma, France; $C_{16}H_{18}N_3SCl$ is the empirical formula of methylene blue. A stock solution of 1000 mg/L was prepared in bi-distilled water. This solution was then diluted to the desired concentration. For the adjustment of pH, additional chemicals of the analytical reagent grade, such as HCl and NaOH, were created.

Fixed-bed column adsorption study: A fixed bed of Pyrex glass column was used for continuous flow adsorption tests to investigate the dynamic performance of sorghum grain husks in eliminating methylene blue from water. A column with an internal diameter of 1.7 cm and a height of 18 cm is shown in Fig. 1. To reach the desired height of the adsorbent bed, a specific amount of RSH was added to the column. One (01) gram of RSH corresponds to a height of 7.3 cm. In order to reduce bed swelling, a section of glass beads and glass wool was positioned at the bottom of the column, and another quantity at the top of the RSH bed. The fixed-bed is powered continuously using a peristaltic pump connected to a tray filled with an aqueous solution of methylene blue. Samples are collected from the column at regular time intervals. The effects of pH, initial methylene blue concentrations

(100, 150, and 200 mg/L), flow rates (1, 2.5, and 5 mL/min), and bed height were investigated in a number of trials. The studies were conducted at a temperature of 25 degrees Celsius. The samples were examined using an OPTIZEN UV/VIS spectrophotometer set at a wavelength of 665 nm.

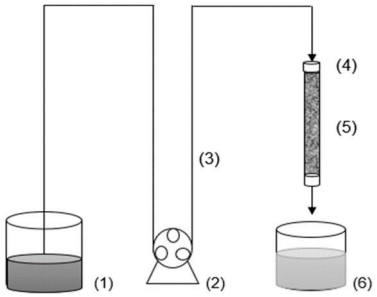

Fig. 1. The experimental set-up, (1) influent container, (2) peristaltic pump, (3) silicon tubing, (4) glass wool, (5) fixed-bed adsorbent, (6) effluent container

Analysis of column data: To obtain different column data values such as: volume of effluent (V_e), breakthrough time (t_b), exhaustion time (t_e), column adsorption capacity (Q_{tot}) and removal percentage (R%), column data analysis was achieved for different experimental breakthrough curves [35]. Breakthrough time (t_b) is the time it takes for the concentration of a methylene blue solution at the column exit to fall below 5% of its initial concentration, measured in minutes [36]. The exhaustion time (t_e) represents the required time period to reach or approach the initial C_0 concentration at the exit of the column [37], given by the following formula [38]:

$$t_e = \frac{V_e}{Q} \quad (1)$$

t_e- exhaustion time (min)
V_e - effluent volume treated at exhaustion state (mL)
Q - flow rate (mL/min)

The adsorption capacity can be used to study and explain the performance of the adsorption column, and can be defined as the amount that is adsorbed per unit mass of RSH until the exhaustion state is reached. It can be calculated by following equation (2) [39]:

$$Q_{Tot} = \int_0^{V_e} \frac{C_0 - C}{m}\, dv \quad (2)$$

Q_{Tot} - total capacity adsorption at exhaustion state (mg/g)
V_S - effluent volume at exhaustion time (mL)
C_0 - concentration of methylene blue at the inlet of the column (mg/L)
C - concentration at the outlet of the adsorption column (mg/L)
m - mass of the adsorbent (g)

The removal percentage (R%) is the ratio between the amount adsorbed (mad) and the total amount of adsorbate passing through the adsorption column (mT). It can be calculated by following the relation [40]:

$$R\% = \frac{m_{ad}}{m_T} 100 \quad (3)$$

R% - removal percentage
m_{ad} - adsorbed amount of methylene blue (mg)
m_T - total amount of adsorbate passing through the adsorption column (mg)

Adsorption-desorption cycle studies: For reusing the adsorbent material several times, a fixed-bed regeneration can be performed using hydrochloric acid to remove Methylene blue adsorbed on the surface of the RSH material and reutilize it again. The two associated processes (Adsorption-desorption) are fundamental in the industrial sphere for economic reasons. At the end of adsorption/desorption cycle experiments, the regeneration efficiency was evaluated by the following equation (4) [41]:

$$E\% = \frac{m_d}{m_{ad}} 100 \quad (4)$$

E% - removal percentage
m_d - desorbed mass of methylene blue (mg)
m_{ad} - adsorbed mass of methylene blue (mg)

Application of dynamic models: To study the properties of experimental breakthrough curves and various factors affecting the adsorption process, a Thomas model was applied to calculate the different constants that characterize this model such as: determination of the rate of methylene blue adsorbate transfer from liquid to solid phase, along with the amplitude of q_0 adsorption and the determination coefficient R^2. The following linear equation (5) characterizes this model [42]:

$$\ln\left(\frac{C_0}{C} - 1\right) = \frac{k_{Th} q_0 X}{Q} - k_{Th} C_0 V_e \quad (5)$$

C_0 - The concentration of methylene blue at the inlet of the column (mg/L)
C - concentration at the outlet of the adsorption column (mg/L)
k_{Th} - Thomas constant (mL/(mg·min))
q_0 - Theoretical adsorption capacity (mg/g)
X - mass of RSH (g)
Q - flow rate (mL/min)
V_e - volume of effluent adsorbed during the adsorption process (L)

Yoon-Nelson model was also used to calculate the several kinetics constants that characterize this model; it is described by a following linear relation [43]:

$$\ln\left(\frac{C}{C_0 - C}\right) = \tau k_{YN} - \frac{k_{YN}}{Q_V} V_e \quad (6)$$

C - concentration at the outlet of the adsorption column (mg/L)
C_0 - concentration of methylene blue at the inlet of the column (mg/L)
τ - time corresponding to 50% adsorption of methylene blue solution (min)
$k_{Y\text{-}N}$ - Yoon Nelson constant (1/min)
X - mass of RSH (g)
V_e - volume of effluent adsorbed during the adsorption process (L)

RESULTS AND DISCUSSION

Adsorbent characterization: *Point of zero charges:* The Fig. 2. represents the variation of ΔpH (which is the difference between final pH values and final pH values) versus initial pH values. The curve shows that the pH of point of zero charge value is equal to 6.2 corresponding to ΔpH equals to zero. At pH < 6.2, the global charge of biosorbent surface is positive, while it is negative at pH > 6.2

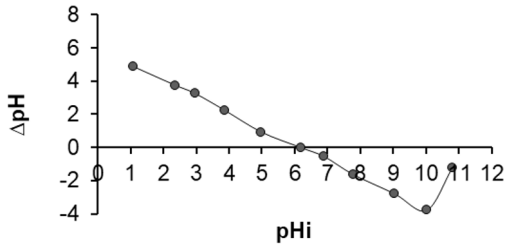

Fig. 2. The variation of pH versus initial pH ($\Delta pH = pH_f - pH_i$)

Fourier transform infrared spectrometry analysis: Fig. 3. depict the Fourier transform infrared (FTIR) spectra of the sample before and after methylene blue adsorption. The band at 3417.98 cm^{-1} is attributed to the stretching vibration of hydroxyl groups (-OH). The peak observed at 2924 cm^{-1} is related to an aliphatic group CH_2 stretching vibration. The N-H/ C-O stretching is responsible for the little peak at 2368.66 cm^{-1}. The asymmetric stretching vibration of C=O is attributed to the peak at 1651.12 cm^{-1}. The peak at 1519.96 cm^{-1} is allocated to aromatic compound or secondary amine groups. The bands at 1373.36 cm^{-1} and at 1342.50 cm^{-1} are attributed to C-H of methyl group. Band at 1041.60 cm^{-1} is attributed to C-O. After the adsorption process some peaks shifted in position (3417.98 to 3441.12 cm^{-1}), (1373.36 to 1388.79 cm^{-1}), and (1041.60 to 1049.31 cm^{-1}), while new peaks appear at 1450.52, 1242.20, 825.56, and 671.25 cm^{-1}. This indicates the formation of new bands between the methylene blue molecule and RSH adsorbent, which suggests the adsorption of methylene blue onto RSH. In light of the changes observed in the spectrum after adsorption, it can be suggested that the hydroxyl and carboxyl groups represent the most important sites for methylene blue adsorption.

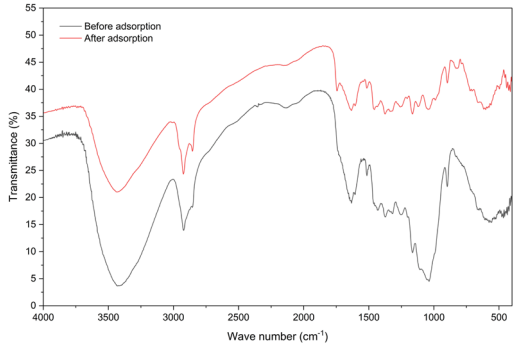

Fig. 3. FTIR spectra of RSH adsorbent before and after adsorption

Scanning electronic microscopy: The SEM analysis shows the high surface morphology of raw sorghum husk adsorbent, which contains the cracks or broad gaps and the pores before adsorption process, as illustrated in Fig. 4. (A), but after process of adsorption, there is only the pore and broad gaps as illustrated in Fig. 4. (B), which explain reducing of methylene blue concentration after adsorption process.

Specific surface area and pore volume: The textural

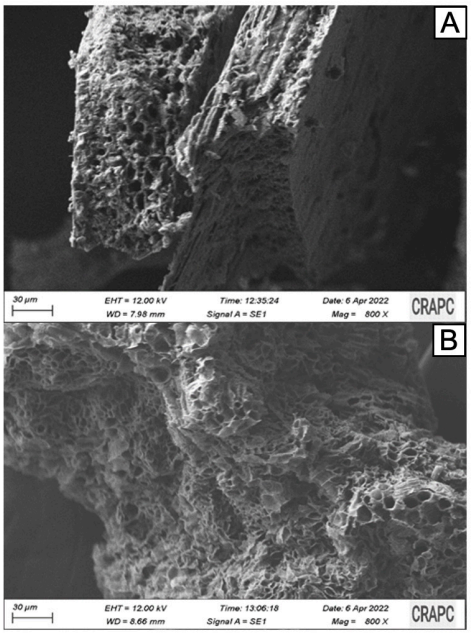

Fig. 4. SEM image of RSH adsorbent, (A) before adsorption, (B) after adsorption

properties of the RSH adsorbent were characterized by nitrogen adsorption-desorption isotherms (Fig. 5). The sample exhibited a BET specific surface area of 30 m^2/g and a total pore volume of approximately 0.2 cm^3/g. The pore size distribution ranged from 2 to 50 nm, indicating a predominantly mesoporous structure according to the IUPAC classification. These results suggest that RSH possesses a well-developed porous network suitable for molecular diffusion and adsorption processes.

Adsorption test: *Effect of pH:* The adsorption of methylene blue solution on the RSH adsorbent is mostly

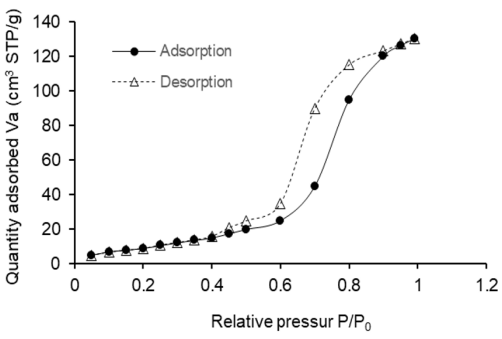

Fig. 5. N_2 adsorption/desorption isotherms for RSH adsorbent

influenced by pH parameter. Therefore, the effect of this factor has been studied by changing pH values from 3 to 8, and other factors, including the solution's initial concentration, the height of the adsorption column, and the value of the flow rate at the entrance of the column, were kept at 100 mg/L, 7.3 cm, and 2.5 mL/min, respectively. The ratio (r) variation represented on Fig. 6. shows that the values of both breakthrough time and exhaustion time increase when moving from the acidic pH (pH = 3) to the alkaline pH (pH = 8), where the time t_b increases from 5 min to 90 min, and exhaustion time t_e from 120 min to 240 min, respectively, indicating that the adsorption of methylene blue solution process is more effective, and more favoured in the alkaline pH solution. With regard to the adsorption capacity, it goes from 1.070 mg/g for pH = 3 to 22.08 mg/g for pH = 8 in the case of the breakthrough point, and from 2.25 mg/g to 39.85 mg/g, respectively, for the saturation point. These results can be explained as follows: for acidic pH, hydronium (H_3O^+) ions are in abundance, and there may be a competition with cationic molecules of methylene blue for adsorption on the RSH surface. However, in the case of the basic medium, the overall charge of RSH is negative, which favours the adsorption of methylene blue which is cationic, similar results have been reported by other researchers [44].

The significant decrease in breakthrough time observed at acidic pH can also suggests that the increase in proton concentration (H_3O^+) simulates an extreme cationic competition condition. These protons compete aggressively with methylene blue cations for the available active sites, thereby accelerating the saturation of the adsorbent bed. Many studies on biosorbents have shown that while other cations (Na^+, Ca^{2+}, Mg^{2+}) can influence adsorption through ionic strength, their impact is often secondary or negligible compared to the dominant effect of pH on surface charge and proton competition [45, 46].

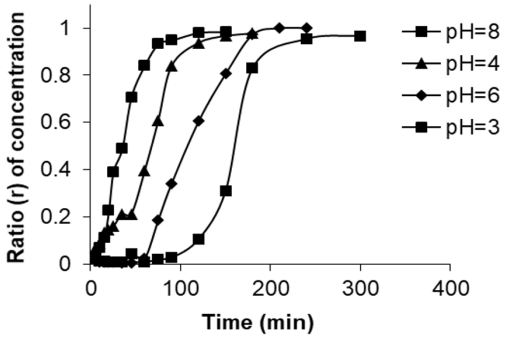

Fig. 6. Effect of pH on adsorption of methylene blue at: C_0= 100 mg/L, H= 7.3 cm, particles diameter: 400-500 μm, Q= 2.5 mL/min, r = C(t)/C_0

Effect of initial concentration: Column experiments were performed by varying the methylene blue concentration from 50 to 200 mg/L at bed height of 7.3 cm, flow rate of 2.5 mL/min and pH of 6.2. Fig. 7. illustrates the breakthrough curves obtained for adsorbate concentration of 50, 100, 150, and 200 mg/L. Experimental results demonstrate that when the initial concentration of methylene blue is low, the breakthrough occurs at a later stage, and the surface of RSH becomes saturated with methylene blue after a considerable duration of time. In contrast, when the concentration of methylene blue is higher, the breakthrough occurs within a short time. The decreased concentration gradient led to a reduced transport velocity due to lower diffusion [25, 27]. Similar findings have been reported by other researchers [27].

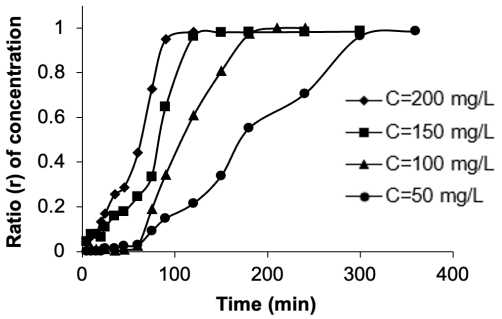

Fig. 7. Effect of initial concentration on adsorption of methylene blue at: pH = 6.2, H= 7.3 cm, particles diameter: 400-500 μm, Q=2.5 mL/min, r = C(t)/C_0

Effect of bed height: The effect of bed height on the adsorption was investigated at pH 6.2. Different adsorbent amounts of 1, 1.5, and 2 g were put in the column to have bed sizes of 7.3, 10.8 and 14.6 cm respectively. The flow rate and concentration of aqueous solution were maintained constant at 2.5 ml/min and 100 mg/L, respectively. Fig. 8. shows the ratio (r) of concentration over time changes for different bed sizes. Specifically, t_b increased from 60 minutes to 120 minutes while t_e extended from 210 minutes to 360 minutes when as the column height was doubled from 7.3 cm to 14.6 cm (i.e., using 1 to 2 g of adsorbent). This means that a taller bed improves the adsorption process. This indicates that the adsorption process is improved with increasing bed height.

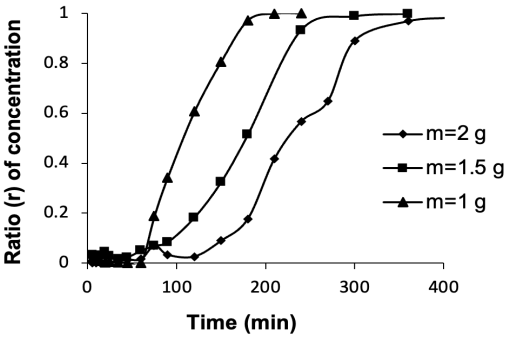

Fig. 8. Effect of bed height on adsorption of methylene blue at: pH=6.2, C_0 = 100 mg/L, particles diameter: 400-500 μm, Q=2.5 mL/min r = C(t)/C_0

These results could be explained as follows: when bed height values increase, the surface area expands; thus, the actives sites of RSH material increase, thereby enhancing the adsorption capacity. Other researchers have reported similar results about the effect of this parameter [45].

Effect of flow rate: In trials using continuous mode, the column's performance is heavily affected by the flow rate. This parameter is crucial when evaluating the effectiveness of the adsorbent in treating wastewater on an industrial or pilot scale. To investigate the impact of the flow rate on the removal of methylene blue dye using raw sorghum husk, the flow rates were adjusted to 1, 2.5, and 5 mL/min. The pH constant was maintained at 6.2, the bed height at 7.3 cm and the methylene blue concentration at 100 mg/L. The results are shown in Fig. 9. The breakthrough time (t_b) and exhaustion time (t_e) decrease from 60 minutes to 25 minutes and from 270 minutes to 120 minutes, respectively, when transitioning from flows with small values (1 mL/min) to flows with large values (5 mL/min). The volume at the breakthrough point (V_b) and at the saturation point (Ve) is 150 mL and 525 mL, respectively. During the initial phase, the adsorption process occurred rapidly, probably due to the presence of sites capable of capturing dye molecules.

During the next phase of the process, when these sites gradually filled up, the uptake became less efficient. The column was able to retain methylene blue dyes even after reaching the point of breakthrough. It was observed that the highest level of adsorption occurred at a flow rate of 1 mL/min, resulting in a percentage removal of approximately 53.72%. The percentage of methylene blue dye removed dropped as the flow rate rose. When the contact time between the methylene blue and RSH is very short due to a high flow rate, it can lower the effectiveness of removal [46]. At a reduced flow rate, methylene blue exhibited an increased duration of contact with the adsorbent. Previous studies on the adsorption of methylene blue dye using melon peels [27], pine cone [35], rice husk [42] and calcined clay [47] have also observed a comparable pattern of results.

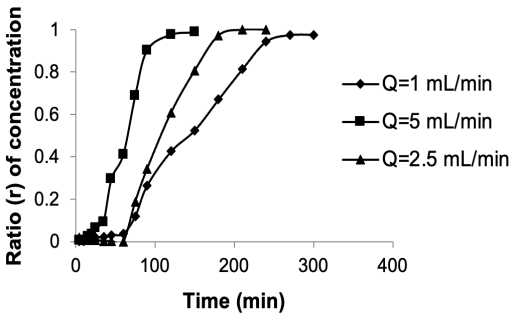

Fig. 9. Effect of flow rate on adsorption of methylene blue at: pH= 6.2, C_0 = 100 mg/L, H= 7.3 cm, particles diameter: 400-500 μm, r = $C(t)/C_0$

Adsorption models application: *Thomas model:* The various parameters of this model were calculated for each of the preceding influential factors, and then organized in Table 1.

Thomas' equation (5) is considered one of the most prevalent models used to fit experimental curves. As indicated in Table 1. the Thomas constant (k_{Th}) rises when decreasing column height and inlet concentration of methylene blue solution.

However higher flow rates values increase the k_{Th}. On the other hand, the theoretical adsorption capacity q_0 rises with increasing of flow rate until reaching a value of 35.04 mg/g at Q equals 5 mL/min. These results indicate that both mass external transfer zone and internal diffusion affect the adsorption kinetic. Additionally, according to the Thomas model, the theoretical adsorption capacity q_0 approaches the experimentally calculated adsorption capacity for the studied experimental conditions like pH values, inlet concentration C_0, flow rate Q and adsorption column height H. For example, when the initial concentration and the volumetric flow rate values are 100 mg/L and 2.5 mL/min respectively, the theoretical capacity q_0 and the experimental capacity values are 42.8 mg/g and 39.86 mg/g respectively. Also, when volumetric flow rate and inlet concentration are 5 ml/min and 100 mg/L respectively, the calculated capacity q_0 and experimental adsorption capacity values are

Table 1. Thomas model parameters under different operating conditions

Different pH conditions at C_0 = 100 mg/L, H = 7.3 cm and Q = 2.5 mL/min				
pH	2	4	6	8
k_{Th} (mL/(mg·min))	0.519	0.391	0.579	0.3
q_0 (mg/g)	10.93	16.75	26.34	42.83
R^2	0.891	0.97	0.958	0.917
Different initial concentration conditions at pH = 6.2, H = 7.3 cm and Q = 2.5 mL/min				
C_0 (mg/L)	50	100	150	200
k_{Th} (mL/(mg·min))	0.296	0.579	0.483	0.304
q_0 (mg/g)	47.30	26.34	17.96	27.056
R^2	0.941	0.958	0.96	0.977
Different bed height conditions at pH = 6.2, C_0 = 100 mg/L and Q = 2.5 mL/min				
H (cm)	7.3	10.8	14.6	
k_{Th} (mL/(mg·min))	0.579	0.288	0.285	
q_0 (mg/g)	26.33	25.69	29.25	
R^2	0.956	0.97	0.945	
Different flow rate conditions at pH = 6.2, C_0 = 100 mg/L and H = 7.3 cm				
Q (mL/min)	1	2.5	5	
k_{Th} (mL/(mg·min))	0.334	0.579	0.719	
q_0 (mg/g)	15.81	26.34	35.05	
R^2	0.946	0.956	0.927	

35.05 mg/g and of 31.54 mg/g respectively. The solution pH affects how well a substance can adsorb.

As pH values increase, the theoretical adsorption capacity q_0, also increases. Whereas, the Thomas's kinetic constant decreases from pH=3 to pH=4. The high determination coefficient R^2 obtained from the model suggests its suitability for analysing experimental data related to experimental curves in various parameters.

Yoon-Nelson model: The numerous parameters of this model were calculated for each of the previous influencers, and then classified in Table 2.

Table 2. Yoon-Nelson model parameters under different operating conditions

Different pH conditions at C_0 = 100 mg/L, H = 7.3 cm, and Q = 2.5 mL/min				
pH	2	4	6	8
k_{Y-N} (1/min)	0.052	0.039	0.056	0.03
τ (min)	43.70	67.18	108.93	171.33
R^2	0.891	0.97	0.956	0.917
Different initial concentration conditions at pH 6.2, H = 7.3 cm, and Q = 2.5 mL/min				
C_0 (mg/L)	50	100	150	200
k_{Y-N} (1/min)	0.019	0.056	0.027	0.061
τ (min)	321.58	108.93	128.15	53.93
R^2	0.764	0.956	0.972	0.977
Different bed height conditions at pH 6.2, C_0 = 100 mg/L, and Q = 2.5 mL/min				
H (cm)	7.3	10.8	14.6	
k_{Y-N} (1/min)	0.058	0.029	0.028	
τ (min)	105.17	153.10	238.21	
R^2	0.956	0.967	0.945	
Different flow rate conditions at pH 6.2, C_0 = 100 mg/L and H = 7.3 cm				
Q (mL/min)	1	2.5	5	
k_{Y-N} (1/min)	0.033	0.058	0.071	
τ (min)	160	105.17	70.98	
R^2	0.946	0.956	0.927	

This model exploits experimental breakthrough curves, where it is observed that the Yon-Nelson constant k_{Y-N} decreases by increasing the height of the adsorption column H and increases by increasing the volumetric flow rate Q as well as the concentration. As the initial concentration C_0 of the methylene blue solution rises from 100 to 200 mg/L, the Yon-Nelson constant k_{Y-N} increases from 0.019 (1/min) to 0.061 (1/min). The time (τ) required to adsorb half of the initial quantity of methylene blue decreases from the initial concentration (50 mg/L) to (200 mg/L). This is because the difference between t_b and t_e shrinks as the initial concentration rises. When the volumetric flow rate increases, the decrease in time (τ) is observed, it goes from 160 min to 71 min going from 1 mL/min to 5 mL/min. As in the case of the Thomas model, the values of the determination coefficients R^2 are very correct.

Column regeneration: To study the effect of regenerating RSH and the possibility of reusing it, three adsorption-desorption cycles were carried out (Fig. 10. and Fig. 11.) During regeneration, the adsorbent was regenerated with hydrochloric acid. Regeneration was carried out over a period of time ranging from 80 min to 130 min, as shown in Fig. 11.

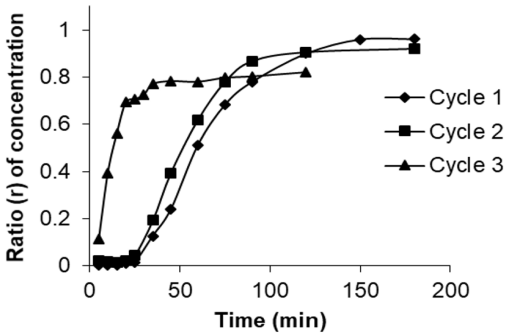

Fig. 10. Breakthrough curves of methylene blue adsorption by RSH adsorbent for three adsorption cycles at: pH= 6.2, C_0 = 100 mg/L, H= 7.3 cm, particles diameter: 400-500 μm, r = C(t)/C_0

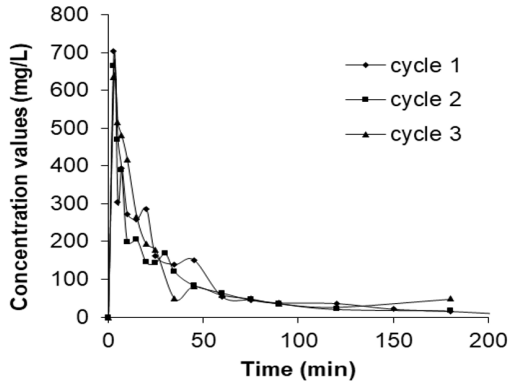

Fig. 11. Methylene blue desorption curves with hydrochloric solution for three cycles

A similar evolution of the three curves representing three consecutive cycles can be noticed. Initially, a high concentration of methylene blue is observed at the column outlet, which then decreases to almost zero. The regeneration efficiency E%, has been calculated for the three cycles, and is 82%, 76%, and 68%, respectively. The ratio between the volume of solution adsorbed during the adsorption phase and the volume of acid used in the regeneration process (concentration factor), was also calculated and the value obtained is 1.56 for the first cycle.

CONCLUSIONS

This work aimed to use sorghum grain husks (RSH) as adsorbents for the removal of methylene blue from aqueous solutions in a fixed-bed column. Specifically, influences of initial pH, initial concentration, bed height, and flow rate were investigated. The results showed that an alkaline pH, a low initial concentration, a high

bed height and a low flow rate favour the adsorption of methylene. The adsorption capacities were satisfying, reaching almost 40 mg/g. Given these promising results, RSH could be a strong alternative to traditional adsorbents such as activated carbon.

AUTHOR CONTRIBUTIONS

AC[1]: designed the research, performed the experiments, analysed the data and contributed to writing, review, and editing of the manuscript; FH, SC and FH: contributed to writing, review, and editing of the manuscript; AC[3]: supervised and advised the overall work; ARY: advised and supervised the overall work; BN: contributed to writing, review, and editing of the manuscript. All authors approved the final version of the manuscript.

CONFLICT OF INTEREST

The authors declare that they have no conflicts of interest related to this study.

ACKNOWLEDGMENT

The authors would like to express their sincere gratitude to the laboratory staff of the Department of Science and Technology Adrar University, for their technical support during the experimental work.

FUNDING

This work did not receive any funding.

REFERENCES

1. Yetgin S., Amlani, M. (2025) Agricultural low-cost waste adsorption of methylene blue and modelling linear isotherm method versus nonlinear prediction. *Clean Technologies and Environmental Policy*, **27**(3), 1205-1225. https://doi.org/10.1007/s10098-024-02928-6
2. Fu F., Gao Z., Gao L., Li D. (2011) Effective adsorption of anionic dye, alizarin red S, from aqueous solutions on activated clay modified by iron oxide. *Industrial and Engineering Chem. Res.,* **50**(16), 9712–9717. https://doi.org/10.1021/ie200524b
3. Bopape D.A., Ntsendwana B., Mabasa F.D. (2024) Photocatalysis as a pre-discharge treatment to improve the effect of textile dyes on human health: A critical review. *Heliyon*, **10**(20), 1-31. https://doi.org/10.1016/j.heliyon.2024.e39316
4. Gohr M.S., Abdelhamid A.I., Elshanshory A.A., Soliman H.M. (2022) Adsorption of cationic dyes onto chemically modified activated carbon: Kinetics and thermodynamic study. *Journal of Molecular Liquids,* 346, 118227. https://doi.org/10.1016/j.molliq.2021.118227
5. Rafatullah M., Sulaiman O., Hashim R., Ahmad A. (2010) Adsorption of methylene blue on low-cost adsorbents: A review, *Journal of Hazardous Materials*, **177**(1–3), 70-80. https://doi.org/10.1016/j.jhazmat.2009.12.047
6. Dawood S., Sen T.K., Phan C. (2019) Performance and dynamic modelling of bio-char and kaolin packed bed adsorption column for aqueous phase methylene blue (MB) dye removal. *Environmental Technology (United Kingdom),* **40**(28), 3762-3772, https://doi.org/10.1080/09593330.2018.1491065
7. El Qada E.N., Allen S.J., Walker G.M. (2008) Adsorption of basic dyes from aqueous solution onto activated carbons. *Chemical Engineering Journal*, **135**(3), 174-184. https://doi.org/10.1016/j.cej.2007.02.023
8. Benhadria N., Hachemaoui M., Zaoui F., Mokhtar A., Boukreris S., *et al.* (2022) Catalytic reduction of methylene blue dye by copper oxide nanoparticles. *Journal of Cluster Science*, **33**(1), 249-260. https://doi.org/10.1007/s10876-020-01950-0
9. Zhang S., Cai M., Wu J., Wang Z., Lu X., *et al*. (2023) Photocatalytic degradation of TiO_2 via incorporating Ti_3C_2 MXene for methylene blue removal from water. *Catalysis Communications,* **174**, 1-9. https://doi.org/10.1016/j.catcom.2022.106594
10. Kurniawan T.A., Mengting Z., Fu D., Yeap S.K., Othman M.H.D., *et al.* (2020) Functionalizing TiO_2 with graphene oxide for enhancing photocatalytic degradation of methylene blue (MB) in contaminated wastewater. *Journal of Environmental Management*, **270**, 110871. https://doi.org/10.1016/j.jenvman.2020.110871
11. Pratama S.A., Purnomo A.S., Asranudin A. (2025) Methylene blue removal using alginate-PVA-*Pseudomonas aeruginosa* biocomposite: Kinetics and biodegradation studies. *Biotechnology Reports,* **47**(25), 1-14. https://doi.org/10.1016/j.btre.2025.e00906
12. Liu L., He D., Pan F., Huang R., Lin H., *et al.* (2020) Comparative study on treatment of methylene blue dye wastewater by different internal electrolysis systems and COD removal kinetics, thermodynamics and mechanism. *Chemosphere*, **238**, 124671. https://doi.org/10.1016/j.chemosphere.2019.124671
13. Shahedi A., Darban A.K., Taghipour F., Jamshidi A. (2020) A review on industrial wastewater treatment via electrocoagulation processes. *Current Opinion in Electro-chemistry*, **22**, 154-169. https://doi.org/10.1016/j.coelec.2020.05.009
14. Han G., Du Y., Huang Y., Wang W., Su S., *et al*. (2022) Study on the removal of hazardous Congo red from aqueous solutions by chelation flocculation and precipitation flotation process. *Chemosphere*, **289**, 133109. https://doi.org/10.1016/j.chemosphere.2021.133109
15. Adelin M.A., Gunawan G., Nur M., Haris A., Widodo D.S., *et al.* (2020) Ozonation of methylene blue and its fate study using LC-MS/MS. *Journal of Physics: Conference Series*, **1524**(1), 1-9. https://doi.org/10.1088/1742-6596/1524/1/012079
16. Huang X., Guida S., Jefferson B., Soares A.

(2020) Economic evaluation of ion-exchange processes for nutrient removal and recovery from municipal wastewater. *Npj Clean Water*, **3**(1), 1-10. https://doi.org/10.1038/s41545-020-0054-x
17. Hube S., Eskafi M., Hrafnkelsdóttir K.F., Bjarnadóttir B., Bjarnadóttir M.Á., *et al.* (2020) Direct membrane filtration for wastewater treatment and resource recovery: A review. *Science of the Total Environment*, 710. https://doi.org/10.1016/j.scitotenv.2019.136375
18. Bouras H.D., Yeddou A.R., Bouras N., Hellel D., Holtz M.D., *et al.* (2017) Biosorption of Congo red dye by Aspergillus carbonarius M333 and Penicillium glabrum Pg1: Kinetics, equilibrium and thermodynamic studies. *Journal of the Taiwan Institute of Chemical Engineers,* **80**, 915–923. https://doi.org/10.1016/j.jtice.2017.08.002
19. Bouras H.D., Benturki O., Bouras N., Attou M., Donnot A., *et al.* (2015) The use of an agricultural waste material from ziziphus jujuba as a novel adsorbent for humic acid removal from aqueous solutions. *Journal of Molecular Liquids,* **211**, 1039-1046. https://doi.org/10.1016/j.molliq.2015.08.028
20. Ceroni L., Benazzato S., Pressi S., Calvillo L., Marotta E., *et al*. (2024) Enhanced adsorption of methylene blue dye on functionalized multi-walled carbon nanotubes. *Nanomaterials*, **14**(6), 522. https://doi.org/10.3390/nano14060522
21. Zhang P., O'Connor D., Wang Y., Jiang L., Xia T., *et al.* (2020) A green biochar/iron oxide composite for methylene blue removal. *Journal of Hazardous Materials*, **384**, 121286. https://doi.org/10.1016/j.jhazmat.2019.121286
22. Huang L., He M., Chen B., Hu B. (2021) Sustainable method towards magnetic ordered mesoporous polymers for efficient methylene blue removal. *Journal of Environmental Sciences* (China), 99(ina), **99**, 168-174. https://doi.org/10.1016/j.jes.2020.06.018
23. Li Y., Zimmerman A.R., He F., Chen J., Han L., *et al.* (2020) Solvent-free synthesis of magnetic biochar and activated carbon through ballmill extrusion with Fe_3O_4 nanoparticles for enhancing adsorption of methylene blue. *Science of the Total Environment,* **722,** 137972. https://doi.org/10.1016/j.scitotenv.2020.137972
24. Gulluce E., Karadayi M., Gulluce M., Karadayi G., Yildirim V., *et al.* (2020) Bioremoval of methylene blue from aqueous solutions by *Syringa vulgaris* L. hull biomass. *Environmental Sustainability*, **3**(3), 303-312. https://doi.org/10.1007/s42398-020-00122-0
25. Yan K.K., Huang J., Chen X.G., Liu S.T., Zhang A.B., *et al.* (2016) Fixed-bed adsorption of methylene blue by rice husk ash and rice husk/$CoFe_2O_4$ nanocomposite. *Desalination and Water Treatment,* **57**(27), 12793-12803. https://doi.org/10.1080/19443994.2015.1052988
26. Hokkanen S., Bhatnagar A., Sillanpää M. (2016) A review on modification methods to cellulose-based adsorbents to improve adsorption capacity. *Water research*, **91**, 156-173. https://doi.org/10.1016/j.watres.2016.01.008
27. Djelloul C., Hamdaoui O. (2015) Dynamic adsorption of methylene blue by melon peel in fixed-bed columns. *Desalination and Water Treatment*, **56**(11), 2966-2975. https://doi.org/10.1080/19443994.2014.963158
28. Gaber M.M., Shokry H., Hassanin A.H., Awad S., Samy M., *et al.* (2025) Novel palm peat lignocellulosic adsorbent derived from agricultural residues for efficient methylene blue dye removal from textile wastewater. *Applied Water Science*, **15**(2), 32. https://doi.org/10.1007/s13201-025-02363-y
29. Sen T.K. (2023) Adsorptive removal of dye (methylene blue) organic pollutant from water by pine tree leaf biomass adsorbent. *Processes,* **11**(7), 1877. https://doi.org/10.3390/pr11071877
30. Bhomick P.C., Supong A., Baruah M., Pongener C., Sinha D. (2018) Pine Cone biomass as an efficient precursor for the synthesis of activated biocarbon for adsorption of anionic dye from aqueous solution: Isotherm, kinetic, thermodynamic and regeneration studies. *Sustainable Chemistry and Pharmacy*, **10**, 41-49. https://doi.org/10.1016/j.scp.2018.09.001
31. Jiang X., Sun P., Xu L., Xue Y., Zhang H., *et al*. (2020) Platanus orientalis leaves based hierarchical porous carbon microspheres as high efficiency adsorbents for organic dyes removal. *Chinese Journal of Chemical Engineering*, **28**(1), 254-265. https://doi.org/10.1016/j.cjche.2019.03.030
32. Gherbia A., Sahel D., Bouabidi A., Chergui, A. (2024) A kinetic and thermodynamic study of cationic thiazine dye removal from aqueous solution by date stones variety ghars: an agricultural waste. *International Journal of Energy Research*, **3**(1), 4644094. https://doi.org/10.1155/2024/4644094
33. Ge H., Wang C., Liu S., Huang Z. (2016) Synthesis of citric acid functionalized magnetic graphene oxide coated corn straw for methylene blue adsorption. *Bioresource Technology*, **221**, 419-429. https://doi.org/10.1016/j.biortech.2016.09.060
34. Belhadi B., Djabali D., Souilah R., Yousfi M., Nadjemi B. (2013) Three small-scale laboratory steeping and wetmilling procedures for isolation of starch from sorghum grains cultivated in Sahara of Algeria. *Food and Bioproducts Processing*, **91**(3), 225-232. https://doi.org/10.1016/j.fbp.2012.09.008
35. Yagub M.T., Sen T.K., Afroze S., Ang H.M. (2015) Fixed-bed dynamic column adsorption study of methylene blue (MB) onto pine cone. *Desalination and Water Treatment*, **55**(4), 1026-1039. https://doi.org/10.1080/19443994.2014.924034
36. Asamoah E.N., Liu H., Fan X. (2025) Fixed-

bed adsorption of methylene blue using granular NaX zeolite/attapulgite composite: efficiency, mechanism and reusability of saturated G-NaX/A. *Separation and Purification Technology*, **354**, 128710. https://doi.org/10.1016/j.seppur.2024.128710

37. Benis K.Z., Sokhansanj A., Hughes K.A., McPhedran K.N., Soltan J. (2023) An engineered biochar for treatment of selenite contaminated water: Mass transfer charac-teristics in fixed bed adsorption. *Chemical Engineering Journal*, **469**, 143946. https://doi.org/10.1016/j.cej.2023.143946
38. Mariyam A., Mittal J., Sakina F, Baker R.T., Sharma A.K. (2021) Fixed-bed adsorption of the dye Chrysoidine R on ordered mesoporous carbon. *Desalination and Water Treatment*, **229**, 395-402. https://doi.org/10.5004/dwt.2021.27382
39. Futalan C.M., Wan M.W. (2022). Fixed-bed adsorption of lead from aqueous solution using chitosan-coated bentonite. *International Journal of Environmental Research and Public Health,* **19**(5), 2597. https://doi.org/10.3390/ijerph19052597
40. Kebir M., Tahraoui H., Chabani M., Trari M., Noureddine N., *et al.* (2023) Water cleaning by a continuous fixed-bed column for Cr (VI) eco-adsorption with green adsorbent-based biomass: an experimental modeling study. *Processes,* **11**(2), 363. https://doi.org/10.3390/pr11020363
41. Daffalla S.B., Mukhtar H., Shaharun M.S., Hassaballa A.A. (2022) Fixed-bed adsorption of phenol onto microporous activated carbon set from rice husk using chemical activation. *Applied Sciences*, **12**(9), 4354. https://doi.org/10.3390/app12094354
42. Sarran M.A., Abdulrazak A.A., Abid M.F., Jawad Albayati A.D., Rashid K.T., *et al.* (2024). Oily wastewater treatment by using Fe_3O_4/bentonite in fixed-bed adsorption column. *Chemengineering,* **8**(5), 92. https://doi.org/10.3390/chemengineering8050092
43. Guo G., Muhammad T., Dolkun A., Gao J. (2024) Fixed-bed adsorption kinetics study of plant total flavonoids based on a flow-injection online spectrophotometric method. *Separation and Purification Technology*, **339**, 126554. https://doi.org/10.1016/j.seppur.2024.126554
44. Patel, H. (2019) Fixed-bed column adsorption study: A comprehensive review. *Applied Water Science*, **9**(3), 45. https://doi.org/10.1007/s13201-019-0927-7
45. Kuang Y., Zhang X., Zhou S. (2020) Adsorption of methylene blue in water onto activated carbon by surfactant modification. *Water,* **12**(2), 587. https://doi.org/10.3390/w12020587
46. Fayoud N., Tahiri S., Alami Younssi S., Albizane A., Gallart-Mateu D., Cervera M.L., Guardia M. (2015) Kinetic, isotherm and thermodynamic studies of the adsorption of methylene blue dye onto agro-based cellulosic materials. *Desalination and Water Treatment*, **48**(1-3), 360-371. https://doi.org/10.1080/19443994.2015.1079249
47. Baaloudj O., Langerame F., Iunnissi R., Buttiglieri G., Del Buono D., *et al*. (2025) Biochar-based downflow fixed-Bed adsorption systems for water rreatment: process optimization, reusability, and techno-economic evaluation. *Separation and Purification Technology*, 134347. https://doi.org/10.1016/j.seppur.2025.134347
48. Alalwan H.A., Abbas M.N., Abudi Z.N., Alminshid A.H. (2018) Adsorption of thallium ion (Tl3+) from aqueous solutions by rice husk in a fixed-bed column: Experiment and prediction of breakthrough curves. *Environmental Technology and Innovation,* **12**, 1-13. https://doi.org/10.1016/j.eti.2018.07.001
49. Khalfa L., Sdiri A., Bagane M., Cervera M. L. (2021) A calcined clay fixed bed ad-sorption studies for the removal of heavy metals from aqueous solutions. *Journal of Cleaner Production*, **278**, 123935. https://doi.org/10.1016/j.jclepro.2020.123935